A TOUGH AND BIOCOMPATIBLE DOUBLE-NETWORK HYDROGEL FOR 3D BIOPRINTING

A Thesis

Presented to the Faculty of the Graduate School

of Cornell University

In Partial Fulfillment of the Requirements for the Degree of

Master of Science

by

Xiao Liu

08/2021

Abstract

In this work, I developed a 3D printable collagen-based double-network (DN) hydrogel, which demonstrated excellent mechanical properties and low cytotoxicity. Collagen fibrils and poly(AAM-co-DMAPS) formed the double network structure and increased the toughness, as well as elastic modulus, to as high as 2,380% and 2,070%, respectively, compared with a pure collagen hydrogel. The fracture energy of DN hydrogels is 1,100% that of the pristine synthetic hydrogel. Through introduction of collagen, the cell viability of DN hydrogels reached 88%, which is 900% higher compared to pristine polymer hydrogel in viability. A human nose model with good resolution was fabricated using the optimized DN resin by DLP 3D bioprinting, which demonstrates the good potential in tissue engineering for articular cartilage.

Biographical Sketch

M.S. 2018-2021 The Department of Materials Science and Engineering, Cornell University

MEng. 2015-2017 Smith School of Chemical and Biomolecular Engineering, Cornell University

B.S. 2011-2015 Department of Material Science, Beijing Institute of Technology

Acknowledgments

I would like to show my deepest gratitude to my advisor Professor Emmanuel Giannelis, who taught me a lot in the academic area and gave me enough time so that I can finish research. Also, I hope to acknowledge Professor Lawrence Bonassar, Prof. Nikolaos Bouklas and Prof. Robert Shepherd. Without their help, I would not have been able to finish this research. I would also like to acknowledge the assistance of Cameron Darkes-Burkey who took the mechanical tests and did the fracture energy analysis in this work and Leigh Slyker who did the cell seeding experiments and contributed greatly to the SEM in this work. Finally, I would like to thank all members in our group. They are all excellent people and gave me a lot of help during my stay.

Preface

This Master's thesis was written from April 2021 to July 2021 and was submitted to the Department of Materials Science and Engineering of Cornell University. This work demonstrates a novel collagen-based double-network hydrogel, which has potential for tissue engineering of articular cartilage.

I would like to express my appreciation to Professor Emmanuel Giannelis and Professor Christopher Ober for their advice and encouragement. I also want to thank all group members from Giannelis' group for their helpful discussions.

07/10/2021

Xiao Liu

Table of Contents

List of Figures

List of Tables

1. Introduction

Articular cartilage, a smooth tissue which covers the ends of bones, provides a low friction surface to facilitate the transmission of loads to the underlying subchondral bones. However, cartilage cannot regenerate after injury or normal wear and tear. It also degenerates by common diseases such as osteoarthritis, which affects approximately 300 million people worldwide. To regenerate or replace the articular cartilage, which is a hydrogel, materials with good mechanical properties and biocompatibility are needed.

Hydrogels are three-dimensional networks formed by crosslinked polymer chains. Because of their high water content, porosity, and attractive properties such as biocompatibility, biodegradability, permeability, and excellent functionality hydrogels represent a promising class of biomaterials. As such they have attracted attention as candidates for tissue engineering for different applications. [1]

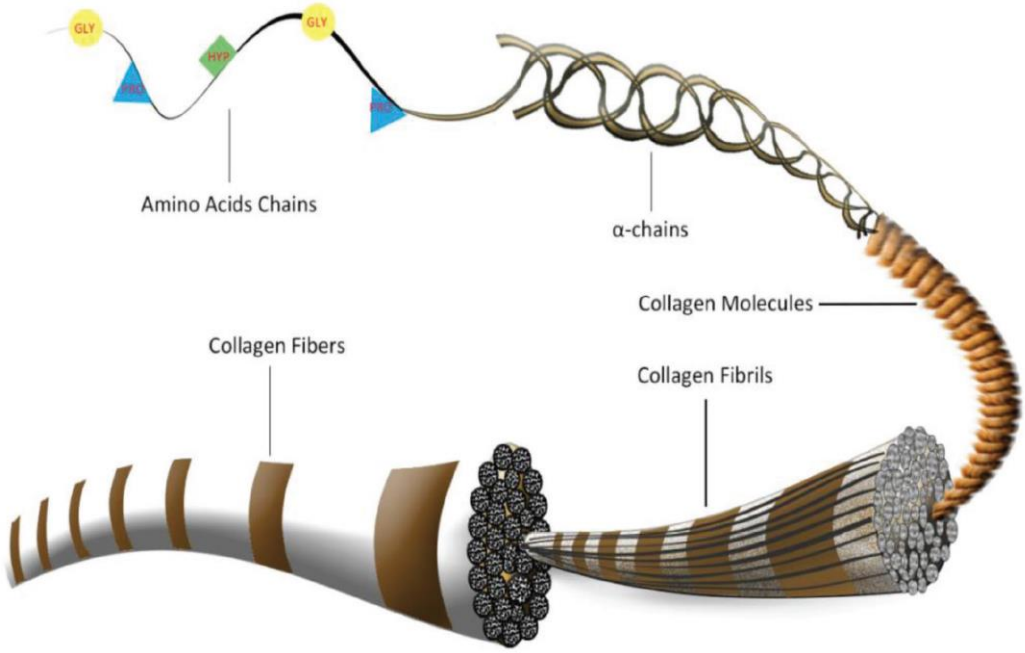

Figure 1. Schematic illustration of the hierarchical structure of a collagen fibril. [2]

As the most abundant protein in the human body, collagen is the key component of the extracellular matrix and constitutes nearly 30% of the body's dry weight. As shown in Figure 1, collagen fibrils have a hierarchical structure, in which collagen molecules consist of a triple helical protein with a characteristic repeating sequence. Collagen plays an important role in cell behavior and biomechanics and provides the ideal environment for cell attachment and proliferation. Because of its structure, collagen shows good biocompatibility, low antigenicity, chemotaxis, flexibility, and good biodegradability. To date, 28 different types of collagen have been identified. However, more than 90% of the collagen in the human body is classified as types I, II and III. Specifically, 90–95% of the collagen in the Extracellular Matrix (ECM) is collagen type II, which helps to stabilize the matrix, providing tensile and shear strength to the articular cartilage. Collagen hydrogels, in which water is the dispersion medium and collagen is the solute, are the most well-studied platforms in tissue engineering. [3] Collagen hydrogels *in vitro* have been studied for tissue engineering and biomedical applications. Bosnakovski et al. fabricated a collagen hydrogel and cultured bone marrow mesenchymal stem cells in collagen type I and II hydrogels. Differentiation was prominent for stem cells in the collagen type II hydrogel, which demonstrated potential for tissue engineering. [4] Achilli et al. studied the effects of pH, ionic strength, and temperature on the gelation behavior of collagen hydrogels. Three to four-fold increases in compressive and tensile moduli were achieved at pH=10, ionic strength of 174 mM and temperature of 4 °C, compared with the control

prepared at neutral pH, ionic strength of 119 mM and 37 °C. [5] Despite this progress, poor mechanical strength still limits their applications as artificial articular cartilage. [6]

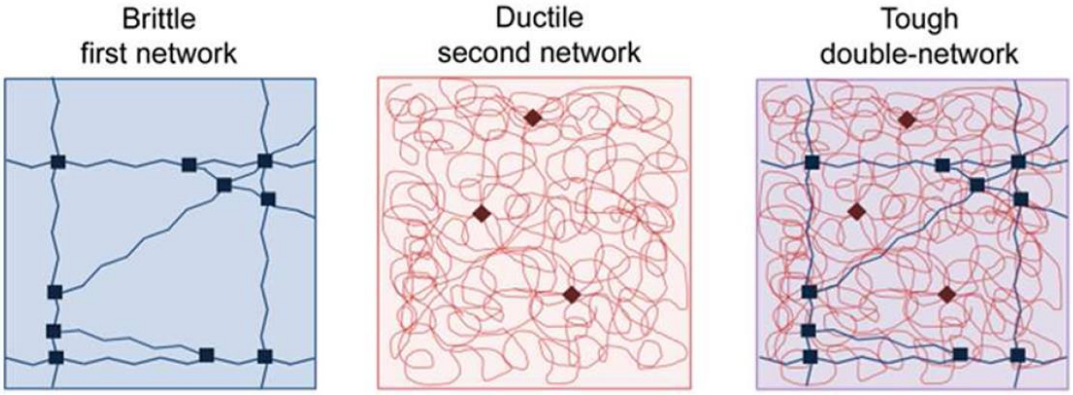

Figure 2. Schematic illustration of the DN structure. [7]

To overcome this limitation, in this study I used a double network (DN) strategy to construct a new family of hydrogels. DN hydrogels show good mechanical properties because of the combination of two networks with complementary structures. As shown in Figure 2, the first network provides sacrificial bonds and will break to disperse the stress surrounding the damage area. The second network is soft and ductile and can sustain large deformation. In 2003, Gong et al. first synthesized PAMPS/PAAm DN hydrogels using a two-step sequential free-radical polymerization process. This DN hydrogel shows a fracture stress of 17.2 MPa, which is 2,000% higher compared to the component single-network gel. [8] However, the irreversible rupture of the covalent bonds upon loading permanently degrades the mechanical properties and, thus, limits its practical applications for repeated loading. Following this work, dynamic and reversible interactions had been introduced into DN materials

to overcome this issue. In particular, strategies such as ionic interactions, hydrogen bonding, dipole-dipole interactions, and chelation have been proposed. Due to this design, recoverable mechanical properties as well as novel properties, such as self-healing, self-gluing and shape memory have been achieved. Zhang et al. developed polyacrylamide (PAAM) / polyvinylpyrrolidone (PVP)/ Ethylene glycol (EG) DN gels and fabricated them as wearable strain sensors. These EG organogels exhibit extreme stretchability of more than 21,000% and high stability. [9] Li et al. synthesized a DN hydrogel based on an ionically cross-linked agar network, a covalently cross-linked acrylic acid (AAC) network. The dynamic and reversible, ionically cross-linked coordination between the AAC chains and Fe^{3+} ions increase the mechanical properties, achieving stretchability up to 3,174.3%, and gauge factors up to 0.83 at a strain of 1,000%. [10] Jia et al. developed a DN hydrogel composed of a polyurethane hydrogel and incorporated dipole−dipole and hydrogen-bonding interactions. This material shows excellent self-healing, self-gluing, and shape-memory properties. [11] In this project, I chose collagen fibrils to form the first network and zwitterionic polymer to form the second network.

Zwitterionic polymers are characterized with both cationic and anionic groups on the polymer repeating units. Because of their good biocompatibility and antifouling properties, zwitterionic polymers are good candidates in drug delivery and tissue engineering. Yuan et al. synthesized zwitterionic polymer-based nanoparticles, which are able to respond to pH changes. Because of the reduced, non-specific protein adsorption of zwitterionic polymers, these nanoparticles show prolonged circulation

time in the body. In response to pH the charge switches to positive, which promotes tumoral cell internalization *in vivo*, resulting in increased inhibition of tumor growth. [12] Zhang et al. fabricated a poly(carboxybetaine methacrylate) hydrogel and implanted it in mice, which resisted the formation of collagenous capsule for at least 3 months and shows good potential for improving the performance of medical devices. [13] In previous research, Pan et al. successfully achieved versatile 3D printable DN hydrogels based on zwitterionic acrylates, using digital light processing (DLP). Due to the addition of zwitterionic molecules, the gelling rate of DN hydrogel was much faster and showed significantly higher G' and G" than its counterpart based on PAAm hydrogels. These hydrogels show a toughness 141.6 kJ/m^3 and good antifouling properties (e.g. the DN hydrogels absorbed significantly less bovine serum albumin). [14]

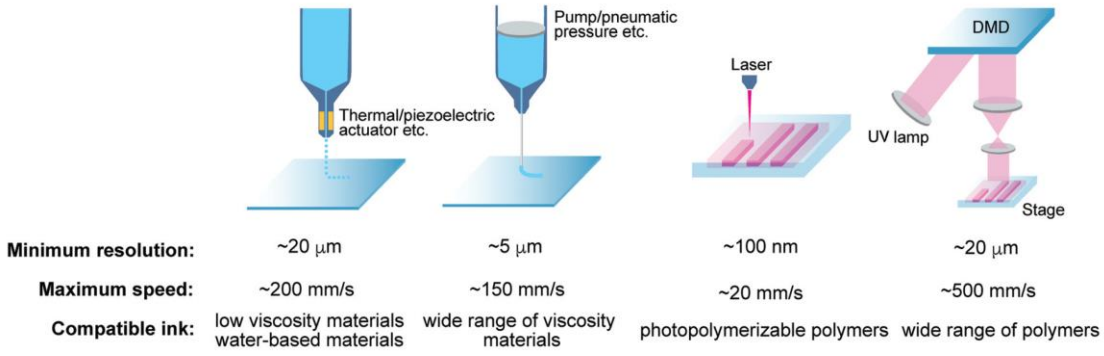

Figure 3. Schematic illustration of four different 3D printing techniques for bioprinting. (a) Inkjet-based 3D printing. (b) Extrusion-based 3D printing. (c) Laser-assisted 3D printing. (d) DLP 3D printing. [15]

In this project, I used 3D bioprinting for fabricating artificial cartilage. Bioprinting, as an emerging research field, has attracted tremendous attention because of its enormous potential applications, such as tissue repair and regeneration, tissue models, and drug delivery. [16-18] Several different bioprinting techniques using collagen-based bioink have already been developed.

One commonly used technique is bioinkjet printing, which uses thermal or acoustic force to eject droplets of bioink onto a substrate in a layer-by-layer fashion to fabricate a 3D structure. Its advantages include low cost and convenience. Lee et al. created a 3D porous scaffold based on collagen, decellularized extracellular matrix (dECM), and silk-fibroin (SF), which shows enhanced mechanical properties and good cell proliferation and differentiation compared to that of the neat collagen scaffold. [19] Another group fabricated a skin equivalent with a layered structure based on collagen, primary human dermal fibroblasts and primary human epidermal keratinocytes. Higher accuracy and uniformity in the distribution of epidermal keratinocytes on the dermal layer and uniform distribution of epidermal layers were achieved. [20] However, major limitations of bioinkjet printing technology include low mechanical properties and a requirement of low-viscosity bioinks to avoid nozzle clogging. In addition, the printing rate is relatively slow.

As the most affordable technique, microextrusion bioprinting uses a controlled pneumatic or physical force to extrude the bioink through a nozzle and deposit it onto a substrate in a layer-by-layer manner to fabricate the 3D structure. As the most

widely used collagen printing technology, it is known for its ease of programming, robust handling, and ability to print multiple cells and materials at a wide range of bioink viscosities. Rhee et al. printed a thermally cured high-density collagen hydrogel using microextrusion bioprinting, which allowed for the deposition of adjacent domains with distinct composition and mechanical properties. [21] Another novel microextrusion bioprinting method was developed by Lee et al. to fabricate an organ-on-a-chip by a simple one-step fabrication process using collagen hydrogel, which achieved low protein absorption and accurate position of heterotypic cell types. [22] In addition, Kim et al. reported a printing strategy combining microextrusion bioprinting with cross-linking to fabricate a 3D porous cell block using a collagen/genipin-bioink, which demonstrated sufficient cell viability, high proliferation and increased osteogenic activities. [23] However, this method typically results in low mechanical strength. It also poses limitations when constructing long and unsupported structures or sharp overhangs. The slow printing speed and low resolution also hamper its applications.

Being a nozzle-free technique, laser-assisted bioprinting (LAB) uses a low energy laser beam to generate bioink droplets from a donor layer and transfers it to a substrate. The main advantages of LAB include high resolution, high cell-seeding density, high cell survival rates, and no nozzle allowing for a wider range of printable bioink viscosities previously limited by nozzle clogging. The tunable energy of the laser pulse also allows accurate positioning of cells and materials at pre-defined location. The separation between the dispenser and bioink limit possible

contamination. Koch et al. used LAB as a multicellular graft to achieve a 3D arrangement of vital cells, which is analogous to native archetype and formed tissue. [24] Michael et al. fabricated a fully cellularized skin substitute using LAB, which formed a 3D skin-like tissue *in vivo*. However, this technology requires rapid gelation kinetics. [25] The powered laser beam may also reduce the cell viability or alter the capacity of cells to communicate and grow in the final tissue construct. Finally, the difficulty to fabricate 3D structures, low throughput rates, high cost, and the inability to move cells to stack them in the Z-direction, limit its widespread application in collagen printing.

Based on the above, a more rapid and versatile printing technique for highly viscous collagen-based resins, with high resolution, smooth surfaces, and desirable resultant mechanical properties is needed. None of the above technologies can achieve these requirements simultaneously. To solve these problems, I selected DLP, which relies on a visible or UV light source to selectively photo-crosslink defined regions of a bioink bath to yield a 3D structure. This method offers much faster printing, smoother surfaces, higher resolution, and the ability to fabricate free-form lattice and patterned structures. To the best of my knowledge, there are no reports of collagen hydrogel printing based on DLP.

In this work, I fabricated a collagen and zwitterion based DN hydrogel and printed a complex human nose model using DLP. The zwitterionic polymer [2-(methacryloyloxy)ethyl]dimethyl-(3-sulfopropyl) ammonium hydroxide (DMAPS)

combined with acrylamide (AAM) and poly(ethylene glycol) diacrylate (PEGDA) formed the first or primary network and collagen fibrils formed the secondary network. Because of this DN structure, a substantial increase in mechanical properties was observed compared to pure collagen hydrogels (e. g. the elastic modulus and toughness of the DN gel are 1,700% and 2,400% higher, respectively, than those of pure collagen hydrogels). The ionic bridging between zwitterionic moieties in the polymer network and zwitterionic moieties with collagen fibrils between the two networks also play an important role in structure stabilization. Polymer chain entanglements between the two networks also contribute to the improved mechanical properties. All together there was an ~1,100% higher fracture energy of the DN hydrogel compared to the single zwitterionic polymer network.

2. Materials and Methodology

2.1. Materials

Acetic acid, acrylamide (AAM, ⩾99%), [2-(methacryloyloxy)ethyl]dimethyl-(3-sulfopropyl) ammonium hydroxide (DMAPS, 95%), hydroquinone, poly(ethylene glycol) diacrylate (PEGDA, M_w 575), phosphate buffered saline (PBS) tablets, 2-acrylamido-2-methyl-1-propanesulfonic acid (AMPS) sodium salt solution (50% wt in H_2O), 0 (SPS, ⩾98%), iron(II) chloride tetrahydrate (98%), iron(III) chloride hexahydrate (⩾98%) and tartrazine were purchased from Sigma-Aldrich Co. (St. Louis, MO). Riboflavin and triethanolamine (TEOHA) were obtained from Neta

Scientific (Hainesport, NJ). Methacrylic acid (MA)was purchased from Tokyo Chemical Industry Co. (Tokyo, Tokyo, Japan). Ammonium hydroxide (29 wt.%) was obtained from Thermo Fisher Scientific Co. (Waltham, MA). All chemicals were used as received without further purification. Millipore Milli-Q water (resistivity > 18 MΩ cm^{-1} at 25 °C) was used in all the experiments.

Collagen was provided by Professor Bonassar's group. It was extracted from rat tail tendons as previously reported. [26] Firstly, rat tail tendons were solubilized in 0.1% acetic acid at 4°C and kept for 48 hours. The concentration of rat tail tendons is 6.67 g/L. Then the supernatant was obtained by centrifugation (9000 rpm, 90 min, 4°C). After that, the supernatant was freeze-dried to get the collagen sponge, which was redispersed in 0.1% acetic acid at a concentration of 30 mg/mL, and stored at 4°C. Iron oxide nanoparticles were synthesized as followed. First, 27 g AMPS sodium salt solution was mixed with 20 mmol MA, 0.71 mmol SPS and dissolve in 200 g Milli-Q water and the solution was stirred at 450 rpm, 65 °C under nitrogen atmosphere for 12 hours. 3. 8 g of the solution was further diluted with 50 g Milli-Q water. Subsequently, 8.88 mmol $FeCl_3 \cdot 6H_2O$ and 4.23 mmol $FeCl_2 \cdot 6H_2O$ were dissolved in this solution under vigorous stirring (600 rpm) at 70 °C under nitrogen atmosphere followed by the addition of 4.286 mL NH_4OH dropwise while continuing the vigorous stirring (600 rpm) at 70 °C under nitrogen atmosphere. The mixture was kept stirring for 30 mins and then left undisturbed at 85 °C for 24 hours under a nitrogen atmosphere.

2.2. Preparation of Collagen-Based Double Network Hydrogels

The chemicals and their amounts used to prepare different samples of the DN hydrogel are summarized in Table 1. A control, single network (SN) sample was also prepared using the same chemicals and method but collagen was not included in the synthesis. AAM, DMPAS, PEGDA, Riboflavin and TEOHA were all dissolved in 10X PBS buffer and Milli Q water. To that solution collagen was added and care was taken to ensure that the highly viscous solution was mixed uniformly throughout. The final concentration of PBS is 1X. 0.187 mmol tartrazine or 20 μm iron oxide nanoparticles solution were added to the solution as light absorbers.

Table 1. Chemicals and their ratios used to prepare 3D printable resins.

Final collagen concentration (mg/mL)	AAM (mmol)	DMPAS (mmol)	PEGDA (mmol)	Riboflavin Solution (0.1% wt) (μL)	TEOHA Solution (30% wt) (μL)	Collagen (g)	10 X PBS (mL)	Milli-Q water (mL)
0	5.63	1.43	0.0730	8	42	0	0.2	0.958
5	5.63	1.43	0.0730	8	42	0.333	0.2	0.597
10	5.63	1.43	0.0730	8	42	0.666	0.2	0.264
15	5.63	1.43	0.0730	8	42	1	0.2	0

2.3. Photorheology Measurement

Photorheology measurements were performed on a DHR3 Rheometer (TA Instrument, New Castle, DE). The wavelength of the light source (Omnicure Series 2000, Lumen dynamics) is 400-500 nm and the power level was set at 100%. The liquid resin was loaded on a 20 mm transparent plate. The frequency of the rheometer was fixed at 1 Hz at a strain of 0.01.

2.4. Scanning Electron Microscope Characterization

The preparation of samples was done by Leigh Slyker. A 4 mm biopsy punch was used to get the samples from the hydrogels, which were incubated for 2 hours at 37°C. A 4% Formalin in PBS solution was used to cross-link the samples for 1 hour. After that, samples were rinsed three times with PBS and two times with Milli-Q water for 10 mins each. Then the samples were cross-linked using 1% osmium tetroxide for 1 hour. A series of ethanol/water (30%, 50%, 70%, 90%, then 100% [x2]) followed by hexamethyldisilazane/ethanol (33%, 50%, 66%, 100% HMDS in ethanol) were used to dehydrate the samples. Gels were dried at room temperature for 12 hours and vacuum dried for 48 hours. After that, samples were attached to sample pins. Silver conductive paint and copper tape were used to increase the conductivity. Finally, samples were sputter coated with Au/Pd alloy for 20 seconds with a current of 20 mA. SEM images were obtained using an accelerating voltage of 0.5 kV and working distance of 5 mm.

2.5. Mechanical Tests

2.5.1 Samples Preparation

Four different samples with different collagen loading (0, 5, 10, 15 mg/mL), among which 0 mg/ml corresponded to the control zwitterionic hydrogel, were prepared. Curing time was tuned based on photorheology data to achieve full curing of the samples.

2.5.1.1 Dog bone samples for tensile test

Sylgard 184 was used to fabricate a transparent ISO 527-2 Type 5A mold with a gauge length of 25 mm and thickness of 2 mm to prepare samples for mechanical testing.

2.5.1.2 Single edge notch samples for fracture energy measurement

The size of rectangular samples with a single edge notch were 7.5 mm × 50mm × 1.5mm. A jig with a razor blade was used to create consistent 2.5 mm cracks at the halfway point of the long side.

2.5.2 Measurements

A Zwick/Roell Z010 testing system (Ulm, Germany) was used to perform the mechanical testing. Because of the nature of the samples, sandpaper was used to provide extra friction to prevent slipping during the testing. Three tests for each condition were run for reproducibility.

2.5.2.1 Tensile tests

For the tensile test, the strain rate was 10 mm/min. Elastic modulus values were calculated from the initial slope of the stress-strain plot up to an engineering strain of 0.05.

2.5.2.2. Fracture energy measurements and calculation

Fracture energy measurements and calculation were done by Cameron Darkes-Burke. The values can be calculated based on the methods from Chen et al. and Tutwiler et al. [27, 28] The values was verified using a method by Tutwiler et al. [28]

2.6. Cell Toxicity Tests

Cell toxicity tests is done by Leigh Slyker. Briefly, samples were rinsed in ethanol and PBS to sterilize the hydrogels. Firstly, the hydrogels were rinsed using ethanol and PBS 6 times for 15 mins each. Then the hydrogels were placed in individual wells in a 24-well plate and primary bovine articular chondrocytes were seeded at a density of 5000 cells/cm^2. The hydrogels were then incubated in Dulbecco's Modified Eagle's Medium (DMEM) with 10% fetal bovine serum at 37 °C for 4 days. Then PBS was used to rinse the hydrogels to wash out DMEM and fetal bovine serum. Calcein AM and Ethidium Homodimer-1 were used to stain the live and dead cells for 20 mins, respectively. PBS was used to wash out Calcein AM and Ethidium Homodimer-1. Then the hydrogels were covered with PBS to prevent drying and immediately imaged on an inverted Zeiss LSM880 confocal microscope with a 10×/0.45 water immersion

objective. For imaging, the wavelength of excitation light was 488 nm and the emission filter for live and dead cells was set at 510-560 nm and 610-660 nm, respectively. A custom MATLAB code was used to count the number of live and dead cells.

2.7. Light Source Curing and 3D Printing

The power of the light source (Omnicure Series 1500, Lumen dynamics) was set at an output of 100% at the wavelength of 400-500 nm. An Ember 3D Printer (Autodesk, San Rafael, CA) was used for printing. 10 mg/mL collagen was added to the zwitterionic resin and the pH was set to 7.5 for 3D printing. The layer thickness was 0.1 mm with an exposure time of 30 s. The human nose model with a length of 12.7 mm, width of 19.88 mm and thickness of 6.57 mm was printed.

3. Results and Discussion

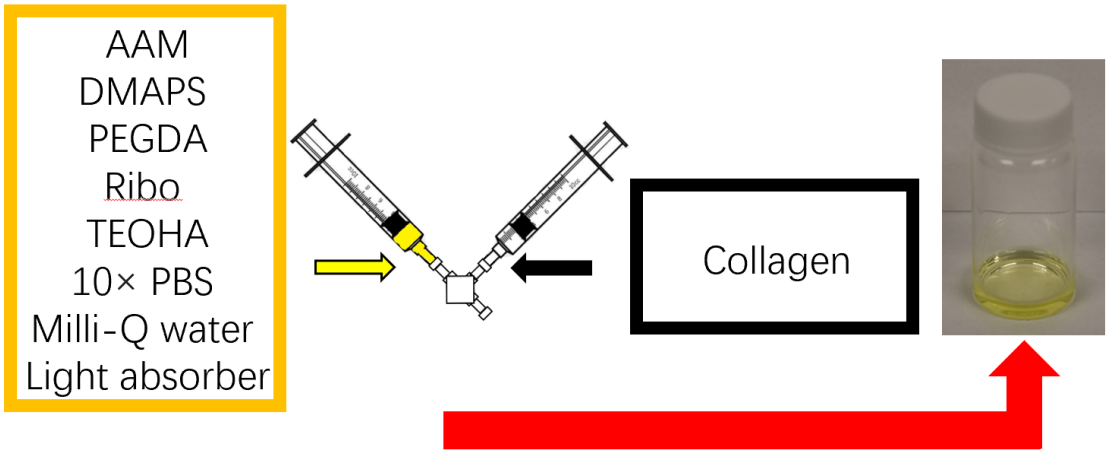

Figure 4. One-step synthesis of the 3D printable resin.

The double network hydrogel (Figure 4) was synthesized using a mixture of AAM and DMAPS (monomers used to form the polymer network), collagen fibrils (second interpenetrating network), PEGDA (chemical crosslinker), Riboflavin (photoinitiator), and TEOHA (co-initiator). Tartrazine or iron oxide nanoparticle were used as light absorbers.

3.1. Chemical Structure

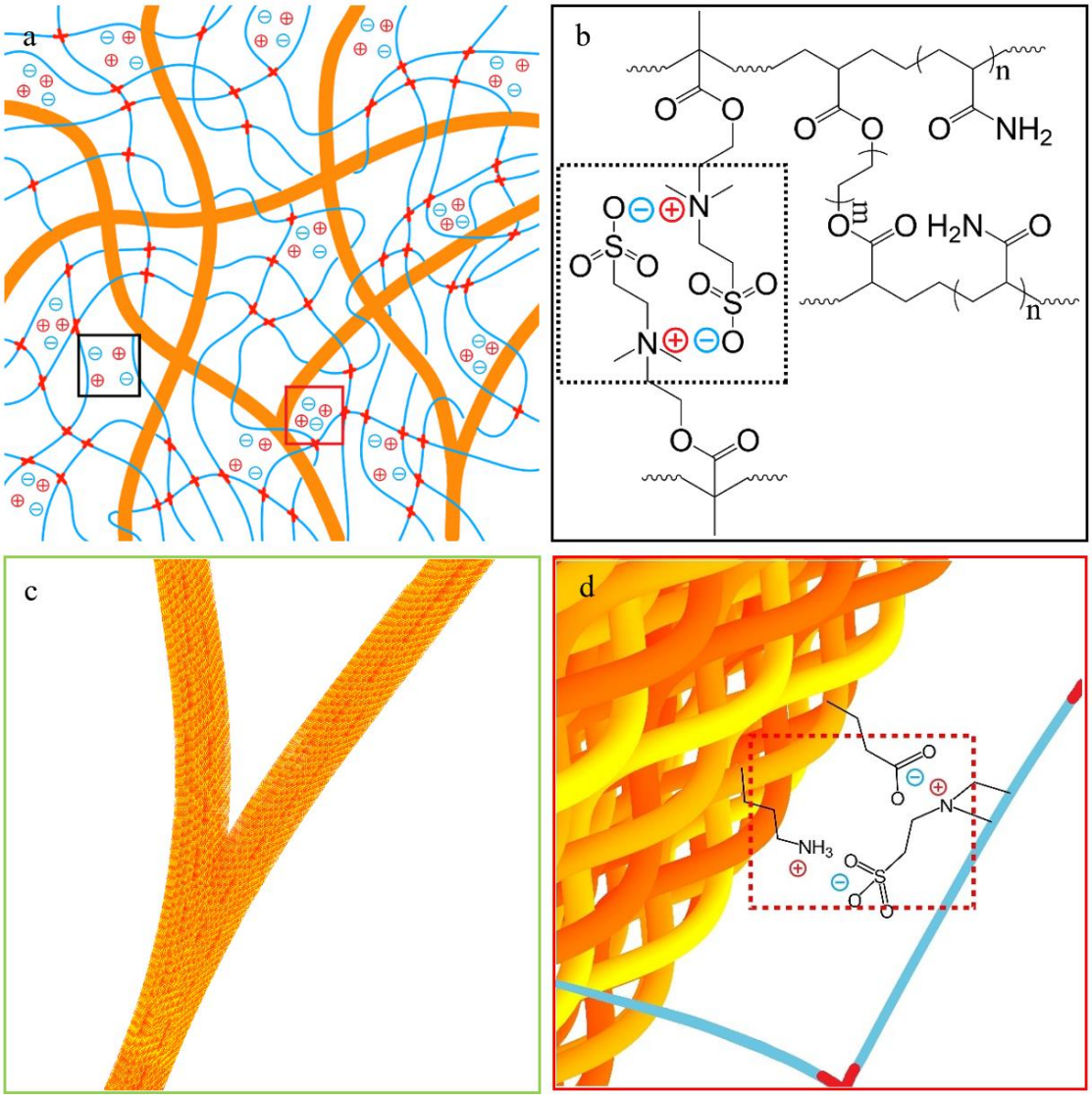

Figure 5. Schematic illustration of DN collagen hydrogel. (a) the DN structure consists of two interpenetrating networks: a collagen network (orange) and a polymer network (blue) (b) The polymer network, showing ionic bonding between the zwitterionic charged groups. (c) The Y branch structure of the collagen fibrils' network. (d) Ionic bridging between the zwitterionic network and the collagen fibril network.

As shown in Figure 5a and 5c, the collagen-based DN consists of two interpenetrating networks: the first network is a poly(AAM-co-DMAPS) and the other consists of the collagen fibril network. Besides the covalent bonds, ionic bonding is also formed in the pristine polymer network and between collagen fibrils and the pristine polymer network because of the charges on the zwitterionic moieties and the collagen, as shown in Figure 5b and 5d. These ionic interactions between ionizable amino acid residues and the hydrogel bound between collagen fibrils also enhance the stability and performance of the hydrogel. [29, 30] Polymer chain entanglement between the polymer network and the network of collagen fibrils may also contribute to the improved performance of the composite.

3.2. Scanning Electron Microscopy Imaging

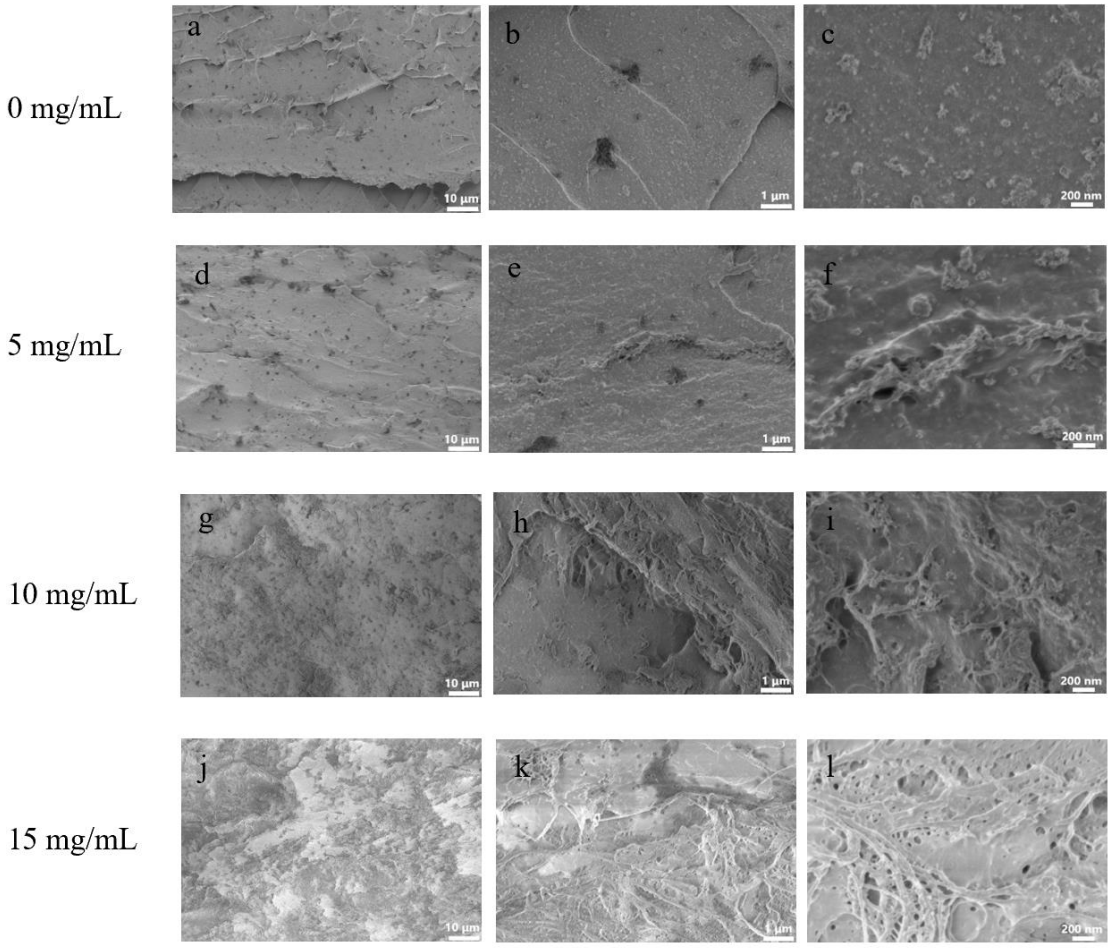

Figure 6. SEM surface images of hydrogel samples containing different amounts of collagen. The concentration of collagen added to the samples is 0 (a-c), 5 (d-f), 10 (g-i), and 15 mg/mL (j-l). The scale bar is 10 micron (left), 1 micron (middle) and 200 nm (right).

Morphology plays a key role in tissue engineering, not only providing mechanical support but also affecting the cell adhesion, proliferation, migration, and

differentiation. [31] SEM images of collagen zwitterionic DN hydrogels confirmed the formation of a collagen fibril network within the hydrogels. Samples containing higher collagen concentrations (10 and 15 mg/mL) show visually increased surface roughness (Figure 6g, 6j) compared to the relatively smoother surfaces of hydrogels with 0 and 5 mg/mL of collagen (Figure 6a, 6d). Increased roughness tends to favor cell colonization and improves the bioactivities of the hydrogel. Fibril-forming collagens have high-avidity ligands for $\alpha 2\beta 1$ integrin, which can mediate cell adhesion and migration. [32, 33] Distinct collagen fibrils can be observed in all gel samples containing 5, 10 and 15 mg/mL collagen (Figure 7e-l).

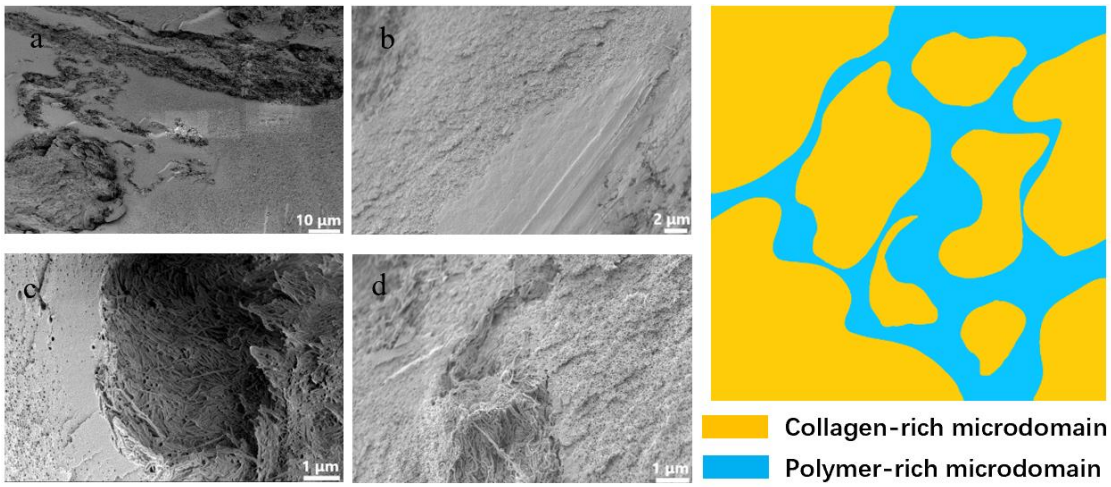

Figure 7. Cross-section SEM images of DN hydrogels. (a-d) The concentration of collagen is 10 mg/mL. (e) Schematic illustration of the structure seen in the images showing the collagen rich (yellow) and polymer rich (blue) domains.

In order to further investigate the morphology of collagen-based DN hydrogels, we sectioned the samples using a razor blade and imaged using SEM. As illustrated in

figure 8a-d, collagen-based DN gels show micro phase separation. One microdomain is collagen-rich while the other is polymer rich (shown in yellow and blue respectively in Figure 7e). Compared to others in the literature these hydrogel composites show smaller domains and better distribution. [34] As shown in Figure 7c, a highly interconnected network with porous and loose structure was formed in the collagen-rich microdomains. The microporous structure is present in both microdomains. These small pores can lead to a higher invasion efficacy, which is important for bioprinting with cells. [35] They also promote cell attachment and proliferation and help with nutrient transport.

3.3. Photorheology

3.3.1 Chemistry Mechanism

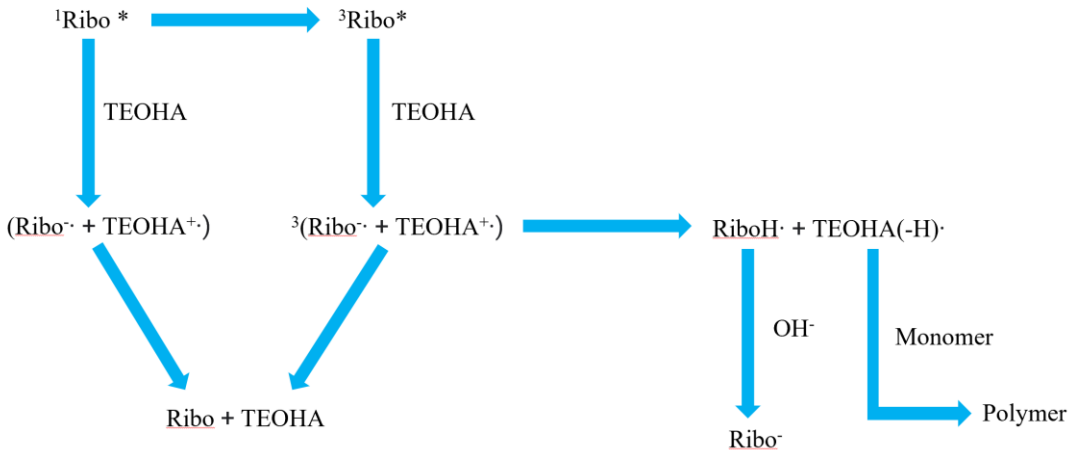

Figure 8 Schematic of the photopolymerization mechanism.

Riboflavin and TEOHA act as the photoinitiator and coinitiator, respectively. Riboflavin and TEOHA were used because of their good biocompatibility. [36] The reported mechanism is as follows. First, Riboflavin forms excited singlet or triplet under light exposure. Then they are quenched by TEOHA and form radicals. Only the radicals formed from triplets are the initiating species leading to polymerization, as shown in Figure 8. [37] The resin used is acidic because of the acidity of DMAPS. To tune the pH to neutral or slightly basic for the photochemistry TEOHA was added and the rates of photopolymerization were studied at different pHs.

3.3.2 Photorheology Measurements

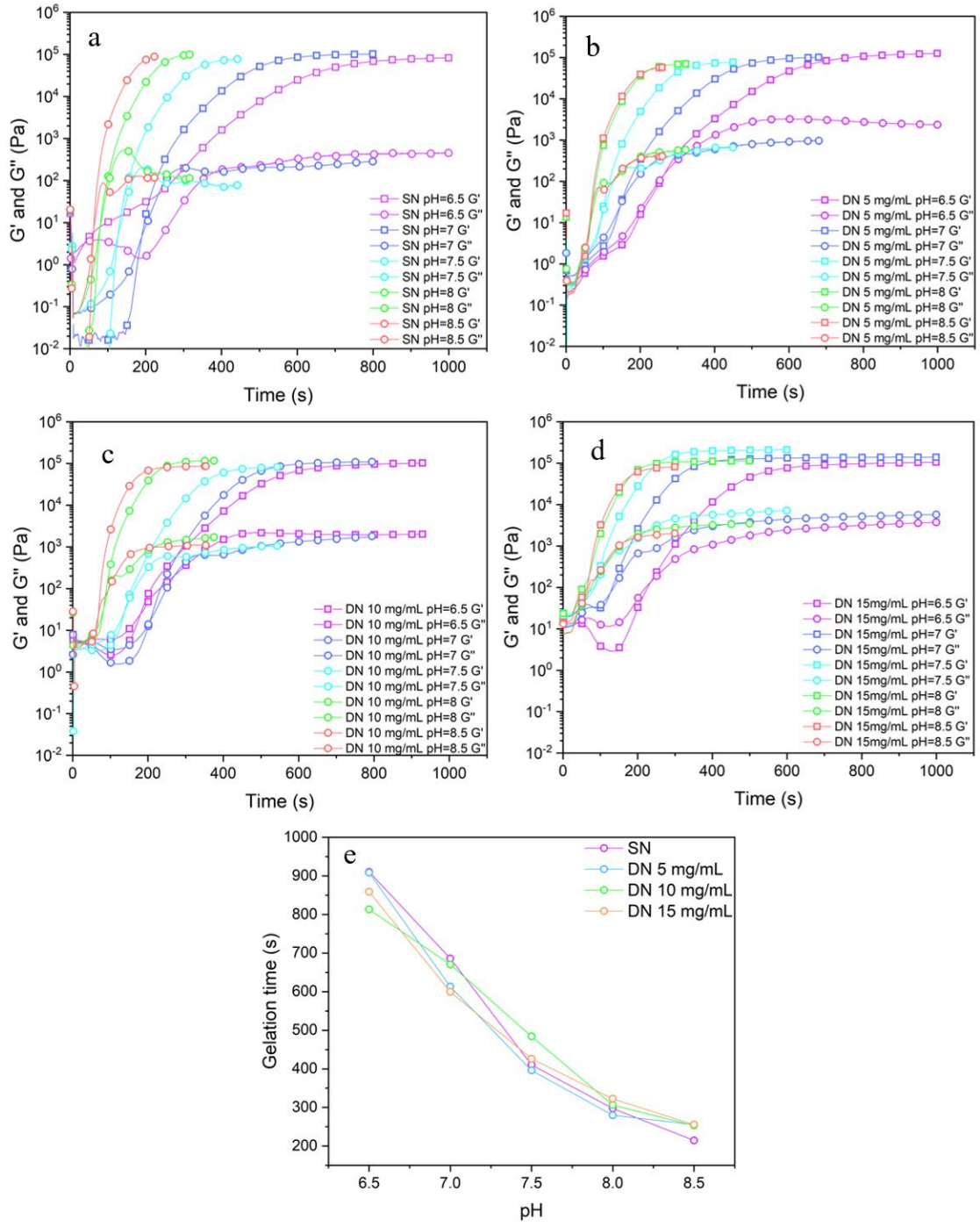

Figure 9. (a-d) Photorheology of hydrogels containing different concentrations of collagen: a) 0 mg/mL, b) 5 mg/mL, c) 10 mg/mL, and d) 15 mg/mL. The pH varied

from 6.5 to 8.5. e) Gelation time for samples with different concentrations of collagen and at different pHs.

As a printing technology featuring high printing speeds and good resolution, DLP requires resins that photocure fast and start at a relatively low viscosity to eventually form solid structures. Photo-rheology is a useful technique to characterize resin printability by monitoring the photo-polymerization as a function of light illumination. As shown in Figure 9a, SN and DN resins have low initial viscosities, which enable a rapid coating of the build layer during DLP printing. For all compositions, the loss modulus (G") is initially higher than the storage modulus (G'); a feature that is characteristic of liquids. As the light is turned on, G' rapidly increases over many orders of magnitude and becomes greater than G'', indicating the transition from liquid to solid. This transformation is faster with higher concentrations of TEOHA indicating that photopolymerization is accelerated at high pH. Gelation time is defined as the time when G' is greater than 95% of the final plateau value. As shown in Figure 9e, when the pH reaches 8, the gelation time is similar for all systems, which implies that further addition of TEOHA did not lead to significant changes of the photopolymerization rate. In addition, the concentration of collagen does not appear to have much of an influence on photopolymerization.

3.4. Mechanical Testing

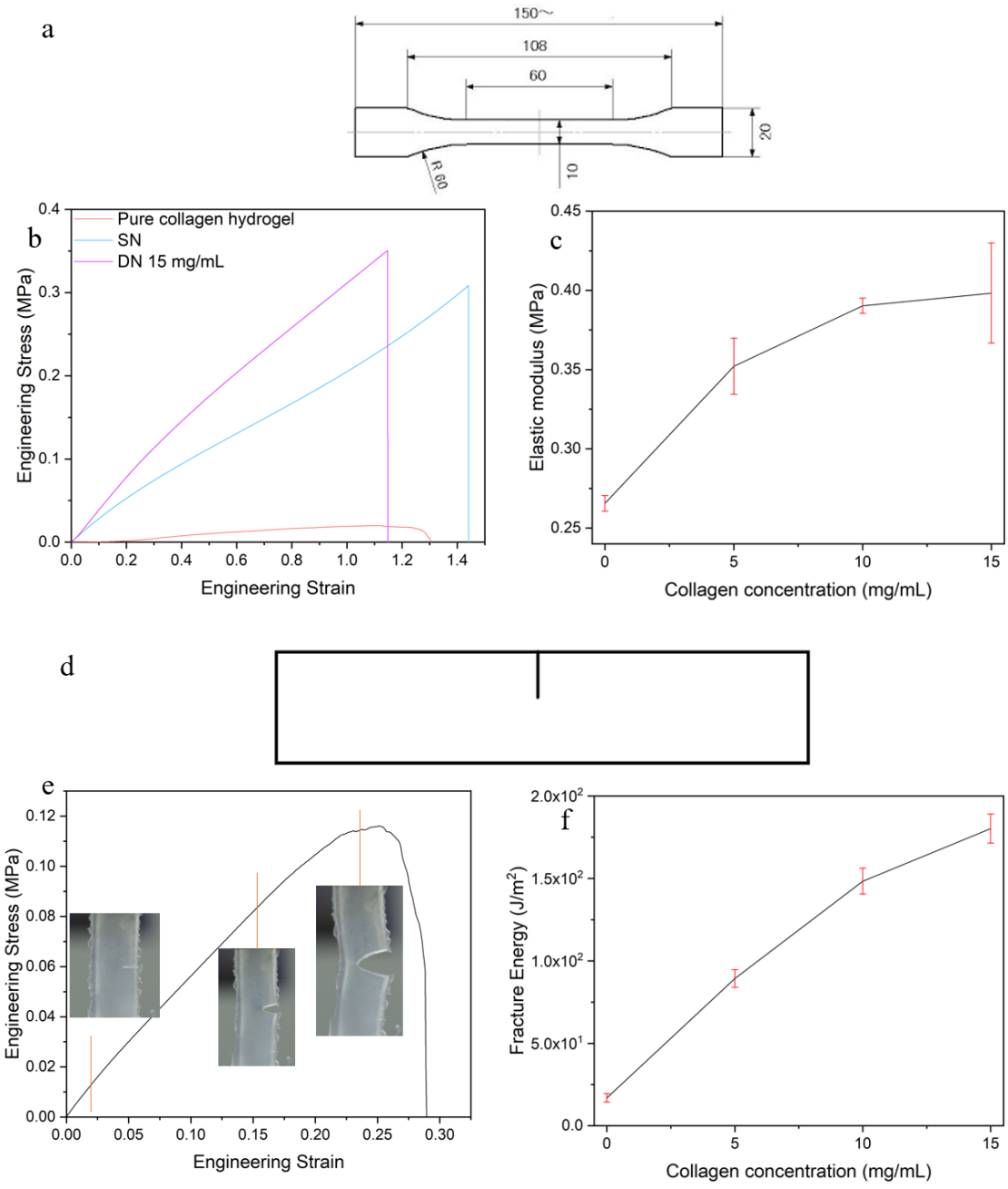

Figure 10. (a) Dog bone sample used for tensile testing. (b) Stress-strain curves of pure collagen hydrogel, pristine polymer hydrogel and collagen-based DN hydrogels. (c) Elastic modulus of collagen-based DN hydrogels with different concentrations of

collagen. (d) Notched sample used for fracture energy experiments. (f) Fracture energy of samples with different collagen concentration.

Two types of tensile test samples were used: a) dog bone samples for elastic modulus and toughness (Figure 10a) measurements, and rectangular coupons with a notch for fracture energy (Figure 10d). Compared with the pure collagen hydrogel (pH 7.5), DN hydrogels with collagen concentration at 15 mg/mL (pH 7.0) show an increase in mechanical properties compared with the single network hydrogel. The toughness of DN hydrogels with 15 mg/mL collagen is 0.2171 MJ/m^3, which is 2,380% higher that of pure collagen hydrogel and 98% of that of the zwitterionic SN hydrogels. The toughness value of the DN hydrogel is similar to that of articular cartilage (0.01-0.8 MJ/m^3). [38] The elastic modulus of DN hydrogels with 15 mg/mL collagen is 2,070% higher compared to the pure collagen hydrogel and 163% of the SN hydrogels but an order of magnitude lower than articular cartilage (7 MPa). [39] The failure strain of DN hydrogels with 15 mg/mL collagen is 80% that of SN hydrogels and is higher than articular cartilage by 25-30%. [39]

Besides elastic modulus and toughness, the fracture energy, or the energy required for an existing sharp crack to propagate, was measured. Fracture energy defines a material's tolerance for pre-existing cracks and other stress concentrators. Articular cartilage, performing in highly dynamic stress environments, may develop small cracks, which propagate and result in a common disease called osteoarthritis. [40] As the target for this project was to fabricate artificial cartilage for potential tissue replacement applications, fracture energy is an important property for the materials.

By comparing fracture energy between samples with different concentrations of collagens, failure resistances between different samples can be compared. Figure 10e shows the engineering stress vs. engineering strain plot of the DN hydrogel with collagen concentration of 15 mg/mL. During the test, the crack propagated as the sample was stretched. As shown in Figure 10f, the fracture energy increased with increasing concentration of collagen. Even at a very low weight fraction (1.5 %), addition of collagen increased fracture energy significantly. The fracture energy of SN hydrogels is 0.017±0.003 kJ/m^2 and well below that of DN hydrogels (0.180±0.009 kJ/m^2), which is within the same order of magnitude of articular cartilage (800 J/m^2) [41] The addition of fibers to the hydrogel enhanced the fracture energy and elastic modulus observed in other hydrogel systems. [42] Compared with other collagen-based hydrogel composites, higher fracture energy and toughness (the latter defined as area under the stress-strain plot) indicates better performance and longer life of the 3D printable DN hydrogels as a potential replacement of artificial cartilage. Moreover, considering the low amount of collagen, this material may also offer a better choice for cost-effective products for wider applications. [18]

3.5. Cell Toxicity Tests

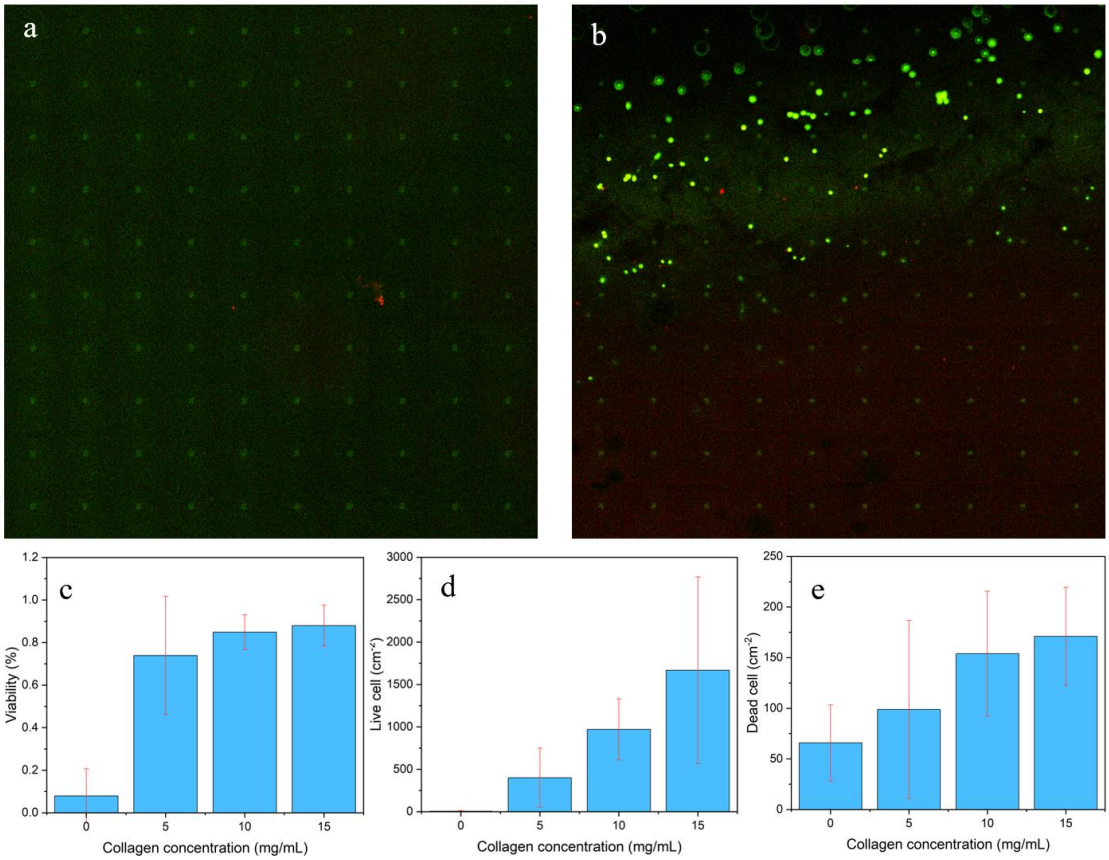

Figure 11. (a, b) Images of live-dead staining of collagen-based DN hydrogels with collagen concentrations of 0 and 15 mg/mL after 4 days of culturing. (c) Cell viability of hydrogels with different concentrations of collagen. (d, e) Number of live and dead cells per square centimeter attached to the hydrogel surface after 4 days. Green dots represent live cells while red dots represent dead cells.

For potential applications as articular cartilage, high cytocompatibility is required. To study the effect of the collagen on cytocompatibility, bovine articular chondrocytes were chosen to seed on the surface of the hydrogels. The cells were cultured for 4 days

and then the live or dead cells were labeled with Calcein AM (green) or Ethidium Homodimer-1 (red), respectively. Confocal microscopy was used to characterize the cell viability and attachment. As shown in Figure 11a, compared with the SN hydrogel, which only showed very few dead cells without any live cells, a much higher number of live cells were observed in the DN hydrogel with very few dead cells 4 days after seeding. The viability of SN hydrogel is 7.9%, and that of DN hydrogel (15 mg/mL) is 88.0% (Figure 11c). The live cell density of DN hydrogel (15 mg/mL) is 1,668 cell/cm^2 compared to 5.264 cell/cm^2 for the SN hydrogel. This indicates that the SN hydrogel has higher cytotoxic effect or weaker cell attachment, while the DN hydrogel has excellent biocompatibility with much better cell attachment. Previous studies showed that collagen contains specific cell binding sites, particularly the RGD amino acid sequence and provides a more biocompatible environment, which leads to increases in biocompatibility and cell attachment of DN hydrogels. [43]

3.6. DLP 3D Printing

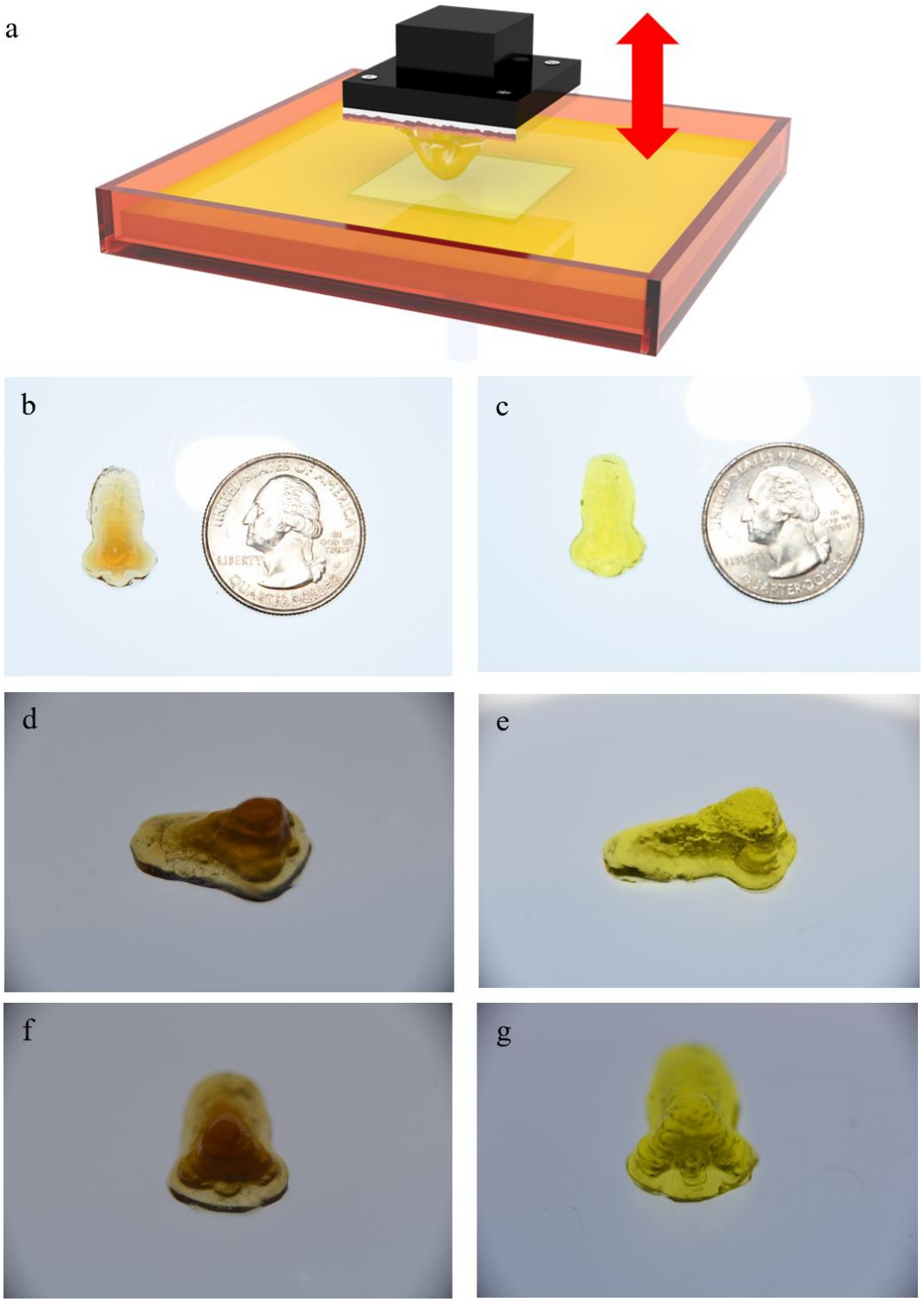

Figure 12. (a,) A schematic overview of the continuous, bottom-up DLP. The arrow indicates the up and down motion used during printing. (b-g) Top, front, and left views of the 3D printed human nose models based on DN hydrogel using DLP with different light absorbers: b, d and f are with iron oxide nanoparticles and c, e, and g are with tartrazine.

As proof of concept a human nose model was printed using DLP. As shown in Figure 12 light passes through a transparent window at the base of a vat and cures a layer of resin. Then, after each layer curing, the build head rise and fall vertically, and resin flows to replenish the build area. Then, the next layer is illuminated, and this process continues. As shown in Figure 12, a human nose model with length of 12.69 mm, width of 19.88 mm and thicknesses of 6.57 mm was printed. Small features such as holes on the nose were preserved demonstrating the high resolution of the printing. The layer thickness is 0.1 mm and the exposure time is 30 s. It took around 30 mins to get the final product, which is much faster than inkjet printing and confirms the high speed of printing process. [44] Typical acrylate photoresins consist of monomers, oligomers, a photoinitiator, and an optical absorber. Iron oxide nanoparticle and tartrazine were used as the light absorber. The function of absorber is to control the penetration depth of the incident light within the print resin and, therefore, the polymerization so as to improve the resolution. The printed model using iron oxide nanoparticles as the absorber had some overcured part and delamination was observed. In contrast, the printed model with tartrazine showed a smooth outer surface without any overcured part, indicating that tartrazine provides better vertical and perpendicular

resolution (Figure 12b-g). Since tartrazine is a low-cost and biocompatible food dye its use is highly advantageous.

4. Conclusions and Recommendations

In this work, a collagen-based DN hydrogel with enhanced mechanical properties and good cytocompatibility was demonstrated. In addition, and as a proof of concept high resolution human nose models based on DLP were fabricated. The DN structure was confirmed by SEM images, which show that the hydrogel consists of two microdomains: a collagen-rich and a polymer-rich. The rate of photopolymerization increases with increasing pH. The fracture energy increases more than 1,000% by the addition of collagen compared with that of SN hydrogels. The addition of collagen increases also the cytocompatibility and cell attachment of hydrogels. The cell viability of DN hydrogels is much higher compared to the SN hydrogels and pure collagen hydrogels. Taken all together the DN collagen hydrogel shows good potential in applications of tissue engineering for articular cartilage, personalized surgical reconstruction and regeneration. [44]

References

[1] Stephanie Fuchs, Alexander U. Ernst, Long-Hai Wang, Kaavian Shariati, Xi Wang, Qingsheng Liu, Minglin Ma, Hydrogels in Emerging Technologies for Type 1 Diabetes, Chem. Rev. 10.1021/acs.chemrev.0c0106 (2020).

[2] Kaili Lin, Dawei Zhang, Maria Helena Macedo, Wenguo Cui, Bruno Sarmento, Guofang Shen, Advanced Collagen-Based Biomaterials for Regenerative Biomedicine, Adv. Funct. Mater. 2019, 29, 1804943

[3] Magdalena Rangel-Argote, Jesu´s A. Claudio-Rizo, Jose´ L. Mata-Mata, Birzabith Mendoza-Novelo, Characteristics of Collagen-Rich Extracellular Matrix Hydrogels and Their Functionalization with Poly(ethylene glycol) Derivatives for Enhanced Biomedical Applications: A Review, ACS Appl. Bio Mater. 2018, 1, 1215−1228

[4] Darko Bosnakovski, Morimichi Mizuno, Gonhyung Kim, Satoshi Takagi, Masahiro Okumura, Toru Fujinaga, Chondrogenic Differentiation of Bovine Bone Marrow Mesenchymal Stem Cells (MSCs) in Different Hydrogels: Influence of Collagen Type II Extracellular Matrix on MSC Chondrogenesis, Biotechnology and Bioengineering. 2006, 93, 1152-1163

[5] Matteo Achilli, Diego Mantovani, Tailoring Mechanical Properties of Collagen-Based Scaffolds for Vascular Tissue Engineering: The Effects of pH, Temperature and Ionic Strength on Gelation, Polymers. 2010, 2, 664-680

[6] Kresanti D. Ngadimin, Alexander Stokes, Piergiorgio Gentile, Ana M. Ferreira, Biomimetic hydrogels designed for cartilage tissue Engineering, Biomaterials Science. 2021, DOI: 10.1039/d0bm01852j

[7] Tiffany C. Suekama, Jian Hu, Takayuki Kurokawa, Jian Ping Gong, Stevin H. Gehrke, Double-Network Strategy Improves Fracture Properties of Chondroitin Sulfate Networks, ACS Macro Lett. 2013, 2, 137−140

[8] Jian Ping Gong, Yoshinori Katsuyama, Takayuki Kurokawa, Yoshihito Osada, Double-Network Hydrogels with Extremely High Mechanical Strength, *Adv. Mater*. **2003**, 15, 1155-1158

[9] Haoxiang Zhang, Wenbin Niu, Shufen Zhang, Extremely Stretchable, Stable, and Durable Strain Sensors Based on Double-Network Organogels, ACS Appl. Mater. Interfaces. 2018, 10, 32640−32648

[10] Huijun Li, Han Zheng, Yu Jun Tan, Shu Beng Tor, Kun Zhou, Development of an Ultrastretchable Double-Network Hydrogel for Flexible Strain Sensors, *ACS Appl. Mater. Interfaces*. **2021**, 13, 12814−12823

[11] Haiyan Jia, Zhangjun Huang, Zhaofu Fei, Paul J. Dyson, Zhen Zheng, and Xinling Wang, Unconventional Tough Double-Network Hydrogels with Rapid Mechanical Recovery, Self-Healing, and Self-Gluing Properties, *ACS Appl. Mater. Interfaces*, **2016**, 8, 31339−31347

[12] You-Yong Yuan, Cheng-Qiong Mao, Xiao-Jiao Du, Jin-Zhi Du, Feng Wang, Jun Wang, Surface Charge Switchable Nanoparticles Based on Zwitterionic Polymer for Enhanced Drug Delivery to Tumor, Adv. Mater. 2012, 24, 5476–5480

[13] Lei Zhang, Zhiqiang Cao, Tao Bai, Louisa Carr, Jean-Rene Ella-Menye, Colleen Irvin, Buddy D Ratner, Shaoyi Jiang, Zwitterionic hydrogels implanted in mice resist the foreign-body reaction, Nat Biotechnol. 2013, 31, 553-556

[14] Wenyang Pan, Thomas J. Wallin, Jeʹreʹmy Odent, Mighten C. Yip, Bobak Mosadegh, Robert F. Shepherd and Emmanuel P. Giannelis, Optical stereolithography of antifouling zwitterionic hydrogels, *J. Mater. Chem. B*, **2019**, 7, 2855--2864

[15] Hiroyuki Tetsuka, Su Ryon Shin, Materials and technical innovations in 3D printing in biomedical applications, J. Mater. Chem. B. 2020, 8, 2930—2950

[16] Murat Guvendiren, Joseph Molde, Rosane M.D. Soares, Joachim Kohn, Designing Biomaterials for 3D Printing, ACS Biomater. Sci. Eng. 2016, 2, 1679−1693

[17] Rod R. Jose, Maria J. Rodriguez, Thomas A. Dixon, Fiorenzo Omenetto, David L. Kaplan, Evolution of Bioinks and Additive Manufacturing Technologies for 3D Bioprinting, ACS Biomater. Sci. Eng. 2016, 2, 1662−1678

[18] Khoon S. Lim, Jonathan H. Galarraga, Xiaolin Cui, Gabriella C. J. Lindberg, Jason A. Burdick, Tim B. F. Woodfield, Fundamentals and Applications of Photo-Cross-Linking in Bioprinting, Chem. Rev. 2020, 120, 10662−10694

[19] Hyeongjin Lee, Gi Hoon Yang, Minseong Kim, JaeYoon Lee, JunTae Huh, GeunHyung Kim, Fabrication of micro/nanoporous collagen/dECM/silk-fibroin biocomposite scaffolds using a low temperature 3D printing process for bone tissue regeneration, Materials Science & Engineering C. 2018, 84, 140–147

[20] Hwa-Rim Lee, Ju An Park, Seongju Kim, Youngmin Jo, Dayoon Kang, Sungjune Jung, 3D microextrusion-inkjet hybrid printing of structured human skin equivalents, Bioprinting. 2021, 22, e00143

[21] Stephanie Rhee, Jennifer L. Puetzer, Brooke N. Mason, Cynthia A. Reinhart-King, and Lawrence J. Bonassar, 3D Bioprinting of Spatially Heterogeneous Collagen Constructs for Cartilage Tissue Engineering, *ACS Biomater. Sci. Eng*. **2016**, 2, 1800−1805

[22] Hyungseok Lee, Dong-Woo Cho, One-step fabrication of an organ-on-a-chip with spatial heterogeneity using a 3D bioprinting technology, *Lab Chip,* **2016**, 16, 2618–2625

[23] Yong Bok Kim, Hyeongjin Lee, Geun Hyung Kim, Strategy to Achieve Highly Porous/Biocompatible Macroscale Cell Blocks, Using a Collagen/Genipin-bioink and an Optimal 3D Printing Process, *ACS Appl. Mater. Interfaces,* **2016**, 8, 32230−32240

[24] Lothar Koch, Andrea Deiwick, Sabrina Schlie, Stefanie Michael, Martin Gruene, Vincent Coger, Daniela Zychlinski, Axel Schambach, Kerstin Reimers, Peter M. Vogt, Boris Chichkov, Skin Tissue Generation by Laser Cell Printing, *Biotechnology and Bioengineering*, **109**, 1855-1863

[25] Stefanie Michael, Heiko Sorg, Claas-Tido Peck, Lothar Koch, Andrea Deiwick2, Boris Chichkov, Peter M. Vogt, Kerstin Reimers, Tissue Engineered Skin Substitutes Created by Laser- Assisted Bioprinting Form Skin-Like Structures in the Dorsal Skin Fold Chamber in Mice, PLoS ONE, 8(3): e57741.

[26] Nicole Diamantides, Louis Wang, Tylar Pruiksma, Joseph Siemiatkoski, Caroline Dugopolski, Sonya Shortkroff, Stephen Kennedy, Lawrence J Bonassar, Correlating rheological properties and printability of collagen bioinks: the effects of riboflavin photocrosslinking and pH, *Biofabrication*. **2017**, 9, 034102

[27] Chao Chen, Zhengjin Wang, Zhigang Suo, Flaw sensitivity of highly stretchable materials, Extreme Mechanics Letters. 2017, 10, 50–57

[28] Valerie Tutwiler, Jaspreet Singh, Rustem I. Litvinov, John L. Bassani, Prashant K. Purohit, John W. Weisel, Rupture of blood clots: Mechanics and pathophysiology, Sci. Adv. 2020; 6 : eabc0496

[29] Neelam Keshwani, Shounak Banerjee, Barbara Brodsky, George I. Makhatadze, The Role of Cross-Chain Ionic Interactions for the Stability of Collagen Model Peptides, *Biophysical Journal*. **2013**, 105, 1681–1688

[30] Fengzhi Jiang, Heinrich Ho¨rber, Jonathon Howard, Daniel J. Mu¨ ller, Assembly of collagen into microribbons: effects of pH and electrolytes, *Journal of Structural Biology*. **2014**, 148, 268–278

[31] Christopher J. Bettinger, Robert Langer, Jeffrey T. Borenstein, Engineering Substrate Topography at the Micro- and Nanoscale to Control Cell Function, *Angew. Chem. Int. Ed.* **2009**, 48, 5406 – 5415

[32] Hongyan Han, Hongyan Ning, Shanshan Liu, Qiang Lu, Zhihai Fan, Haijun Lu, Guozhong Lu, David L Kaplan, Silk Biomaterials with Vascularization Capacity, *Adv. Funct. Mater*. **2016**, 26, 421–432

[33] Jyrki Heino, The collagen family members as cell adhesion proteins, *BioEssays*. **2007**, 29, 1001–1010

[34] MinSeong Kim, Geun Hyung Kim, Electrohydrodynamic direct printing of PCL/collagen fibrous scaffolds with a core/shell structure for tissue engineering applications, *Chemical Engineering Journal*. **2015**, 317–326

[35] Katja Franke, Jiranuwat Sapudom, Liv Kalbitzer, Ulf Anderegg, Tilo Pompe, Topologically defined composites of collagen types I and V as in vitro cellculture scaffolds, *Acta Biomaterialia*. **2014**, 10, 2693–2702

[36] Alexander K. Nguyen, Roger J. Narayan, Two-photon polymerization for biological applications, *Materials Today*. **2017**, 20, 314-322

[37] B. Orellana, A. M. Rufs, and M. V. Encinas, The Photoinitiation Mechanism of Vinyl Polymerization by Riboflavin/ Triethanolamine in Aqueous Medium, *Macromolecules*, **1999**, 32, 6570-6573

[38] David Taylor, Niamh O'Mara, Eoin Ryan, Michael Takaza, Ciaran Simms, The fracture toughness of soft tissues, *Journal of the Mechanical Behavior of Biomedical Materials*, **2012**, 6, 139-147

[39] Yoshihiro Sasazaki, Roger Shore, Bahaa B. Seedhom, Deformation and failure of cartilage in the tensile mode, *J. Anat*. **2006**, 208, 681–694

[40] Kresanti D. Ngadimin, Alexander Stokes, Piergiorgio Gentile, Ana M. Ferreira, Biomimetic hydrogels designed for cartilage tissue engineering, *Biomater. Sci*. **2021**, 9, 4246–4259

[41] N. K. Simha, C. S. Carlson, J. L. Lewis, Evaluation of fracture toughness of cartilage by micropenetration, Journal of Materials Science: Materials in Medicine. 2004, 15, 631–639

[42] Widusha R.K. Illeperuma, Jeong-Yun Sun, Zhigang Suo, Joost J. Vlassak, Fiber-reinforced tough hydrogels, *Extreme Mechanics Letters*. **2014**, 1, 90–96[44] Susan L. Bellis, Advantages of RGD peptides for directing cell association with biomaterials, *Biomaterials*. **2011**, 32, 4205-4210

[43] Mihyun Lee, Riccardo Rizzo, František Surman, Marcy Zenobi-Wong, Guiding Lights: Tissue Bioprinting Using Photoactivated Materials, *Chem. Rev*. **2020**, 120, 10950−11027

[44] Mihyun Lee, Riccardo Rizzo, František Surman, Marcy Zenobi-Wong, Guiding Lights: Tissue Bioprinting Using Photoactivated Materials, *Chem. Rev*. **2020**, 120, 10950−11027